

XMM-Newton CCF Release Note

XMM-CCF-REL-285

EPIC-pn FW Closed Offset Maps for Timing and Burst Modes

M.J.S. Smith, M. Guainazzi, M. Freyberg, R. Saxton

May 23, 2012

1 CCF Components

Name of CCF	VALDATE	EVALDATE	Blocks Changed	XSCS Flag
EPN_TICLOSEDODI_0001	1999-12-10T00:00:00	2003-01-26T12:46:06	MASTER_CLOSED_OFFSET	NO
EPN_TICLOSEDODI_0002	2003-01-26T12:46:07	2003-07-25T01:15:40	MASTER_CLOSED_OFFSET	NO
EPN_TICLOSEDODI_0003	2003-07-25T01:15:41	2004-01-12T13:44:35	MASTER_CLOSED_OFFSET	NO
EPN_TICLOSEDODI_0004	2004-01-12T13:44:36	2004-05-29T04:41:12	MASTER_CLOSED_OFFSET	NO
EPN_TICLOSEDODI_0005	2004-05-29T04:41:13	2004-08-22T22:57:35	MASTER_CLOSED_OFFSET	NO
EPN_TICLOSEDODI_0006	2004-08-22T22:57:36	2004-11-18T17:05:46	MASTER_CLOSED_OFFSET	NO
EPN_TICLOSEDODI_0007	2004-11-18T17:05:47	2004-11-24T16:42:14	MASTER_CLOSED_OFFSET	NO
EPN_TICLOSEDODI_0008	2004-11-24T16:42:13	2004-11-30T16:19:14	MASTER_CLOSED_OFFSET	NO
EPN_TICLOSEDODI_0009	2004-11-30T16:19:15	2005-10-11T19:37:17	MASTER_CLOSED_OFFSET	NO
EPN_TICLOSEDODI_0010	2005-10-11T19:37:18	2009-02-27T08:21:50	MASTER_CLOSED_OFFSET	NO
EPN_TICLOSEDODI_0011	2009-02-27T08:21:51	2011-12-03T11:19:17	MASTER_CLOSED_OFFSET	NO
EPN_TICLOSEDODI_0012	2011-12-03T11:19:17	2012-03-02T05:01:14	MASTER_CLOSED_OFFSET	NO
EPN_TICLOSEDODI_0013	2012-03-02T05:01:14		MASTER_CLOSED_OFFSET	NO
EPN_BUCLOSEDODI_0001	1999-12-01T00:00:00	2002-09-20T21:15:49	MASTER_CLOSED_OFFSET	NO
EPN_BUCLOSEDODI_0002	2002-09-20T21:15:50	2003-07-13T02:05:35	MASTER_CLOSED_OFFSET	NO
EPN_BUCLOSEDODI_0003	2003-07-13T02:05:36	2004-07-16T01:32:55	MASTER_CLOSED_OFFSET	NO
EPN_BUCLOSEDODI_0004	2004-07-16T01:32:56		MASTER_CLOSED_OFFSET	NO
EPN_BUCLOSEDODI_0005	2008-09-18T19:35:11		MASTER_CLOSED_OFFSET	NO

2 Changes

This set of CCFs contains EPIC-pn Timing and Burst Mode offset maps performed with the filter wheel in CLOSED position during the course of the mission. There is one offset map per CCF, contained in the MASTER_CLOSED_OFFSET block. The respective offset map Observation ID and Revolution Number for each of the CCF issues is shown in the following table:

Name of CCF	Revolution Number	Observation ID
EPN_TICLOSEDODI_0001	0503	0125910901
EPN_TICLOSEDODI_0002	0644	0125321001
EPN_TICLOSEDODI_0003	0683	0154150401
EPN_TICLOSEDODI_0004	0817	0165160201
EPN_TICLOSEDODI_0005	0820	0165160301
EPN_TICLOSEDODI_0006	0904	0202760201
EPN_TICLOSEDODI_0007	0907	0202760301
EPN_TICLOSEDODI_0008	0910	0202760401
EPN_TICLOSEDODI_0009	0913	0202760501
EPN_TICLOSEDODI_0010	1227	0412780101
EPN_TICLOSEDODI_0011	2150	0611181001
EPN_TICLOSEDODI_0012	2239	0656580201
EPN_TICLOSEDODI_0013	2241	9224100002
EPN_BUCLOSEDODI_0001	0409	0112450201
EPN_BUCLOSEDODI_0002	0611	0145841001
EPN_BUCLOSEDODI_0003	0705	0154150501
EPN_BUCLOSEDODI_0004	0980	0213080101
EPN_BUCLOSEDODI_0005	2236	0611181301

3 Scientific Impact of this Update

Analysis has shown a large number of fast mode (i.e. Timing Mode and Burst Mode) observations has been affected by X-Ray Loading (XRL, Smith 2005); see Guainazzi et al. 2011. The SAS task `epreject` has been modified (version 5.14.3) to mitigate the consequences of XRL. For details on the implementation and algorithm see the documentation for `epreject`. However, essentially the method is as follows.

The level of XRL is determined by comparing the exposure offset map with an archival Timing (or Burst) Mode offset map which was calculated with the filter wheel in CLOSED position. An offset value larger than the median difference between the two will be assumed to be due to XRL and the energy scale of events associated with this offset will be corrected accordingly.

Due to temporal variations of the instrumental offset values (see Section 4) the CLOSED offset map used in this comparison should be as close as possible in time to the exposure in question. Hence a set of CLOSED offset maps covering various epochs of the mission is contained in this release of CCFs.

4 Estimated Scientific Quality

Figs. 1 and 2 show the time evolution of, respectively, Timing Mode and Burst Mode CLOSED offset maps (one offset map per panel). Per CCD column, the difference of the mean offset with respect to the median offset across the sample is depicted. Both modes show long-term systematic trends in the mean column offset values. In addition, several columns show variations which are larger than those of the overall envelopes: the columns at the chip edge, and columns 42 to 44 (using the RAWX = [0..63] convention).

In order to minimise the introduction of systematic errors in the XRL correction, the CLOSED offset map being used should be the closest in time to the exposure undergoing correction.

An estimate of the systematic errors introduced in the offset correction can be made by determining the differences of the mean per-column offset values of two consecutive CLOSED offset maps, and comparing these with the median of the differences. This is depicted in Figs. 3 and 4 for Timing and Burst Modes respectively.

In Timing Mode, the excessively varying columns mentioned above show large differences in several cases, ranging from -4 to $+10$ ADU (in EPIC-pn, 1 ADU is equivalent to 5 eV). For the other columns, and for most of the successive pairs of offset maps, the resulting differences in column offset values are within ± 1.5 ADU. However, offset maps taken in revolutions 0913, 1227 and 2150 show larger variations, of up to ± 3 ADU.

Similarly, in Burst Mode the differences are dominated by the excessively varying columns with values which range from -3 to $+6$ ADU. Excluding these, the overall column differences are within ± 1 ADU.

Assuming a smooth temporal trend in instrumental offsets, these values may be used as upper limit estimates of the systematic errors in column offsets which are introduced when correcting an exposure using archival CLOSED offset maps. As spectra are in general extracted from regions of several CCD columns in width, these errors would need to be properly weighted in the spectral analysis.

5 Test Procedures and Summary of the Test Results

Correct format and integrity confirmed with `fverify`. Functional testing with `cifbuild`. Results of an XRL correction test using `epreject` version 5.14.2 are presented in the CCF Release Note of EPN_REJECT_0006.CCF (Guainazzi et al., 2012) and in the SAS v. 12 Science Validation Report (Gabriel et al., in preparation).

6 Expected Updates

These CCFs need only be used in conjunction with fast mode observations performed with a non-CLOSED offset map (e.g. with the filter wheel in THIN, MEDIUM or THICK positions). In the near future it is foreseen that fast mode exposures will be performed by default using offset maps calculated with the filter wheel in the CLOSED position. Hence, XRL will not be an issue in those observations. Until that time, the CCF set will be expanded to contain any additional fast mode offset map performed with the CLOSED filter.

7 References

- Guainazzi, M., et al., 2011, XMM-SOC-CAL-TN-0083
Guainazzi, M., et al., 2012, XMM-CCF-REL-284
Smith, M.J.S., 2005, XMM-SOC-CAL-TN-0050

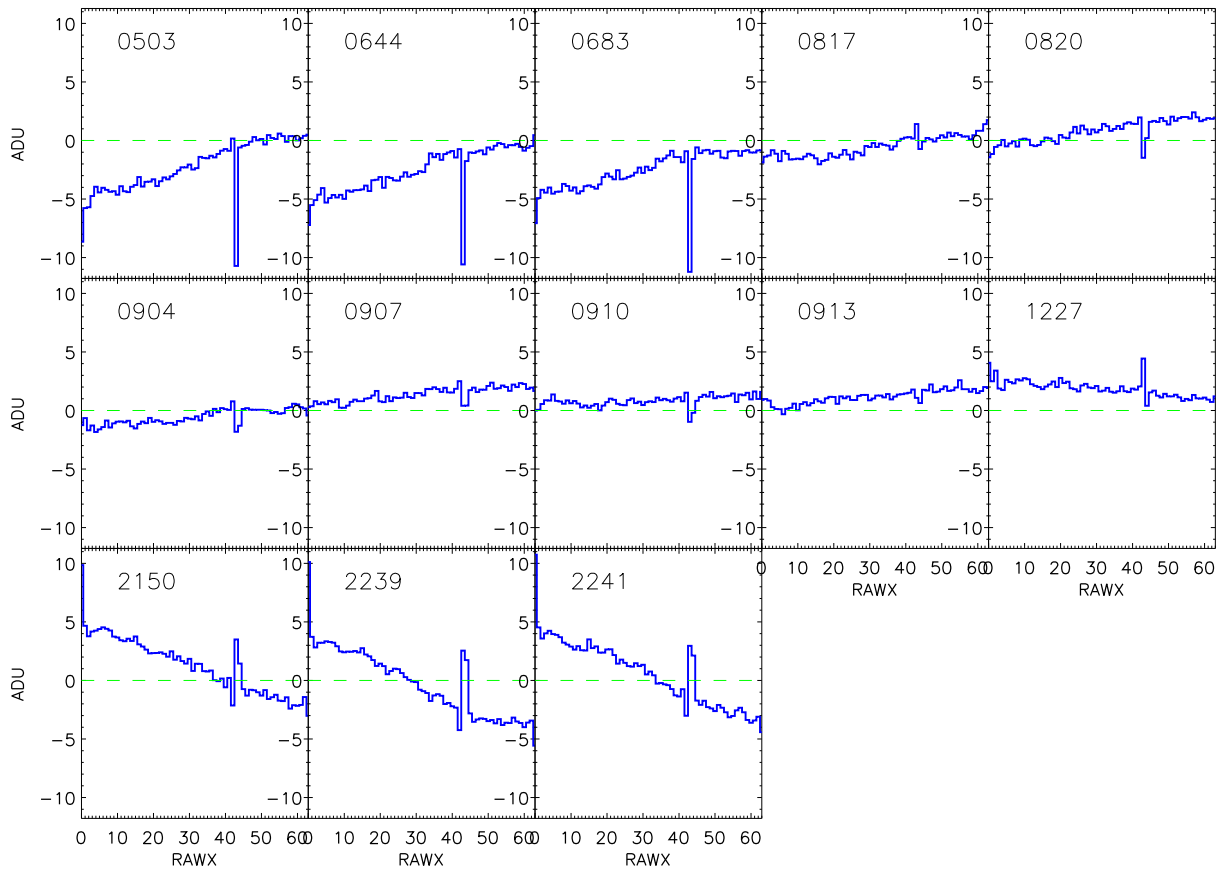


Figure 1: Time evolution of the Timing Mode CLOSED offset maps: column-wise mean offset difference with respect to the median offset of the complete sample, one panel per Timing Mode CLOSED offset map. The panels are ordered chronologically, left-to-right, top-to-bottom, with the respective offset map indicated by the revolution number. On top of the expected random exposure-to-exposure variation there is a clear long-term systematic trend in column offset values. Several individual columns (most notably 0, and 42 – 44) show larger variations.

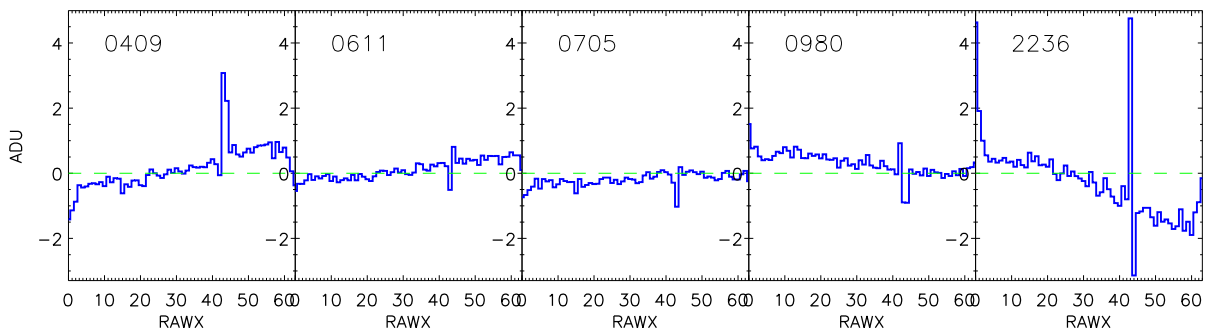


Figure 2: Time evolution of the Burst Mode CLOSED offset maps: analogous to Fig. 1. The long-term systematic trend in column offset values is similar to that seen in Timing Mode. In Burst Mode, columns 0 – 2, 42 – 44 and 62 – 63 show larger variations.

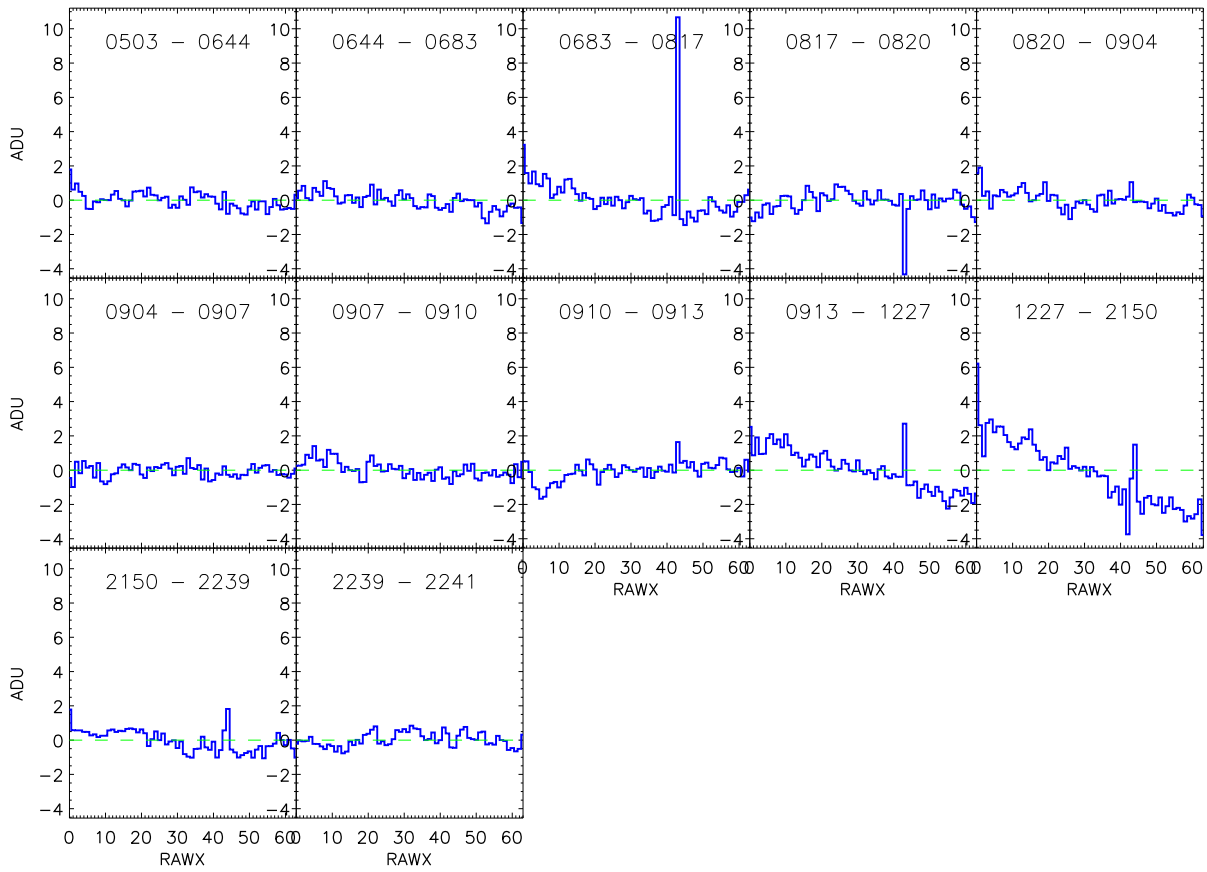


Figure 3: Column-wise mean offset difference (median corrected) between two consecutive Timing Mode CLOSED offset maps. The respective offset maps are indicated by the revolution numbers, and are ordered chronologically as before (see Fig. 1). Assuming a smooth temporal trend in the variation of the overall envelope, this gives an estimate of the maximum error in column offset which may be introduced by applying an archival CLOSED offset map to an observation within the respective revolution range.

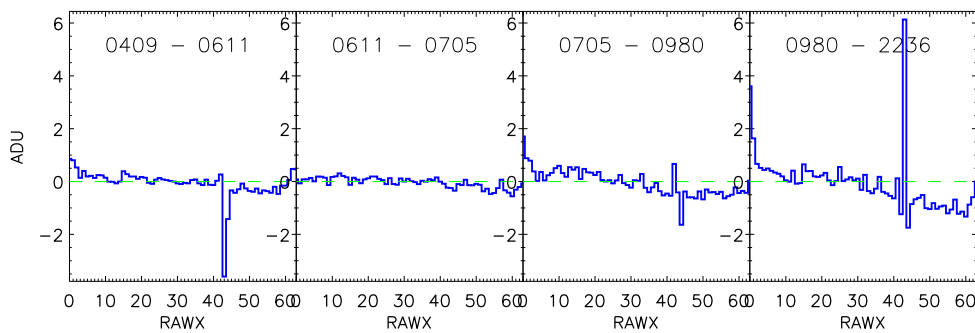


Figure 4: Column-wise mean offset difference (median corrected) between two consecutive Burst Mode CLOSED offset maps, analogous to Fig. 3.